scientific reports

OPEN

Spatiotemporal variations of air pollutants based on ground observation and emission sources over 19 Chinese urban agglomerations during 2015–2019

Tianhui Tao[1], Yishao Shi[1✉], Katabarwa Murenzi Gilbert[1] & Xinyi Liu[2]

The "comparative attitude" of urban agglomerations involves multidimensional perspectives such as infrastructure, ecological protection, and air pollution. Based on monitoring station data, comparative studies of multispatial, multitimescale and multiemission pollution sources of air quality on 19 urban agglomerations during the 13th Five-Year Plan period in China were explored by mathematical statistics. The comparison results are all visualized and show that clean air days gradually increased and occurred mainly in summer, especially in South and Southwest China. $PM_{2.5}$, PM_{10} and O_3 were still the main primary pollutants. $PM_{2.5}$ is mainly concentrated in December, January and February, and PM_{10} is mainly concentrated in October–November and March–April. The O_3 pollution in the Pearl River Delta and Beibu Gulf urban agglomerations located in the south is mainly concentrated from August to November, which is different from others from May to September. Second, from 2015 to 2019, the increasing rate of O_3 concentration in any hour is higher than that of particulate matter (PM). Diurnal trends in O_3 concentration in all directions also showed a single peak, with the largest increments that appeared between 13:00 and 16:00, while the spatial distribution of this peak was significantly regional, earlier in the east but later in the west. Third, this analysis indicated that the annual average air quality index (AQI) showed a gradually decreasing trend outward, taking the Central Plain urban agglomeration as the center. The ambient air pollutants are gradually moving southward and mainly concentrated in the Central Plains urban agglomeration from 2015 to 2019. Furthermore, in each urban agglomeration, the cumulative emission of $PM_{2.5}$ is consisted of the four average emissions, which is approximately 2.5 times of that of PM_{10}, and industries are the main sources of $PM_{2.5}$, PM_{10} and VOCs (volatile organic compounds). VOCs and NO_x increased in half of the urban agglomerations, which are the reasons for the increase in ozone pollution. The outcomes of this study will provide targeted insights on pollution prevention in urban agglomerations in the future.

In global ecological protection and urban development, air pollution has become a crucial issue affecting human health and the environment, along with climate change, which has attracted increasing attention from scholars and government administrators[1–4]. The number of air pollutants has grown from dozens to hundreds now. Major phenomena, such as acid rain, ozone holes, and urban heat islands, continuously challenge the airways of urban dwellers and sustainable urban development[5,6]. After decades of efforts by developed countries in Europe and America, sulfur pollution and soot pollution in urban air have basically been solved, and the environmental air quality has been greatly improved. However, the contribution of NO_x to environmental acidification is growing as the tropospheric ozone problem is aggravated by the emission of nitrogen oxides (NO_x) and volatile organic compounds (VOCs)[7]. In recent decades, the enormous emissions of airborne particulate pollution have become the primary cause of climate change and air pollution in China[8]. Air pollution has gradually changed from a local problem to a regional problem and may be either emitted directly (primary pollutants) or formed in the atmosphere[9]. Major metropolises have invested large human and financial resources to control

[1]College of Surveying and Geo-Informatics, Tongji University, Shanghai 200092, China. [2]Zhejiang Zhipu Engineering Technology Limited Company, Huzhou 313000, Zhejiang, China. ✉email: shiyishao@tongji.edu.cn

1

particulate pollution, but the effect is still unsatisfactory. CO, NO$_x$, hydrocarbons and photochemical smog pollution remained serious.

Urban agglomeration (UA) is a crucial phenomenon at the urban scale and form in the process of globalization. In different stages of socioeconomic and human development, scholars use different terms to describe this urban landscape phenomenon, such as megalopolis[10], urban clusters[11], metropolitan chain areas[12], urban agglomerations[13], metropolitan interlocking regions[14] and conurbations[15]. Despite the inconsistency in terminology, this extensive, multicentered, multicity urban landscape has been well recognized. Urban agglomerations (UAs) in China are dynamic regions with immense potential for regional development, which play a vital role in global competition and the international division of labor and gather many industries, transportation and residents, and the mechanisms of environmental pollution are more complicated[8,16]. Recently, in China, air pollution incidents have changed from frequent occurrence to visible improvement. Meanwhile, the characteristics and influencing factors of air quality have attracted the attention of many researchers[17–19]. Together these results indicate that the spatiotemporal patterns of air pollution are not only related to meteorological conditions such as terrain[20], temperature[21], and humidity[22], but also to the emissions of local and surrounding cities, exhibiting distinct regional features [23]. For example, source contributions to PM$_{2.5}$ indicate that coal[24], biomass burning[25], transport[26] and industry[27] are the main sources.

Only three air pollutants, SO$_2$, NO$_2$ and PM$_{10}$, were monitored, and the air pollution index (API) was calculated by the China National Environmental Monitoring Centre before 2013. Then, China promulgated the Ambient Air Quality Standard (GB3095-2012), adding three indicators, PM$_{2.5}$, CO, and O$_3$, for air quality evaluation. The air quality index (AQI) was used to evaluate the air quality, which makes the air quality evaluation more accurate and strict. At present, China's air quality evaluation indicators are mainly PM$_{2.5}$, PM$_{10}$, SO$_2$, NO$_2$, CO and ozone. However, in terms of identifying regions with similar air pollution behaviors and locating emission sources, few studies have comprehensively considered the spatiotemporal comparison of primary pollutants among UAs and detailed emission sources. For many countries, without this comprehensive assessment, it is impossible to understand the synergies and interrelationships between energy-related urban sprawl and air pollution. Previously published studies on spatiotemporal variations in PM$_{2.5}$ and O$_3$ have mainly focused on a specific region in China (Beijing-Tianjin-Hebei, Yangtze River Delta, or Pearl River Delta) and shorter observation times, ignoring UAs with weak economic development, such as northwest and central China[28–30]. Few studies have compared the changes in pollutant concentrations and primary pollutants in multiple UAs. Six air pollutants and 19 UAs were considered comprehensively in our work. Regional joint prevention and control of air pollution should be strengthened. As China has entered the 14th Five-Year Plan period, it is necessary to review and summarize the air quality situation of China's key UAs in the 13th Five-Year Plan (FYP) and study the impact of anthropogenic emission sources generated in urban construction on air pollution. This is a research highlight of this paper. Given these facts and based on air quality monitoring data, this study aims to investigate (1) the temporal variation characteristics of primary air pollutants in 19 UAs during China's 13th Five-Year Plan period, (2) the spatial distribution features of the barycenter of six ambient air pollutants from 2015 to 2019, (3) the dissimilarity of the contribution of atmospheric pollutants produced by anthropogenic sources at the UA scale.

This paper is organized as follows. In the first stage, we described the study area and the datasets used in the study. Then, we will present the spatial–temporal variation characteristics of primary pollutants based on UAs and anthropogenic source emissions. Finally, we summarized key research findings and drew conclusions.

Study area and methods

China's urban agglomerations. Due to the compound and regional features of air pollution, UAs are the main unit of joint prevention and control of air pollution. UA development planning in China can be divided into world-class, national and regional levels. The 19 selected Chinese UAs from south to north and from west to the east are Beibu Gulf, Pearl River Delta, Central Yunan, Central Guizhou, Chengdu-Chongqing, Triangle of Central China, Central Plains, West Side of the Straits, Yangtze River Delta, Shandong Peninsula, Tianshan North-Slope, Lanzhou-Xining, Guanzhong Plain, Ningxia Yanhuang, Hohhot-Baotou-Ordos-Yulin, Taiyuan-Jinzhong, Beijing-Tianjin-Hebei, Mid-southern Liaoning and Harbin-Changchun UAs. Nineteen UAs locations and names are annotated with colors and numbers in Fig. 1. Moreover, for convenience of expression, Table 1 briefly lists the basic indicators of the 19 UAs in China.

Data sources and statistical analyses. Real-time daily hourly concentrations in each monitoring site covering 19 UAs (Table 2) were derived from China's National Environmental Monitoring Centre. In addition, city daily data (excluding detailed sites) were also used for verification. In this study, the monitoring data were pretreated with python language programming based on Spider platform to ensure the effectiveness of air pollutant concentration data. First, some outliers, such as hourly pollutants concentrations in each station less than zero and missing values, were removed. Secondly, the daily average value of each pollutant in each station was only calculated when the valid data of the day in each station is greater than or equal to 20 h. And the number of effective monitoring points shall not be less than 75% of the total number of urban points. Then the daily mean value (i.e., arithmetic mean of a 24-h monitoring value on a natural day) of urban pollutants can be obtained by calculating the average of each pollutant at each station. Finally, month and annual mean pollutants concentrations for the monitoring sites and UAs were obtained according to the arithmetic mean method[31]. Comparing the annual average concentration of the city with the government report, our calculation results were found to be reliable.

It is well known that 2020 is the year for China to fight the COVID-19 pandemic with all their strengths[32]. Home isolation was adopted to reduce mobility, and social and economic development stagnated. Meanwhile, anthropogenic activities such as transportation and industry are directly proportional to air pollution. Therefore,
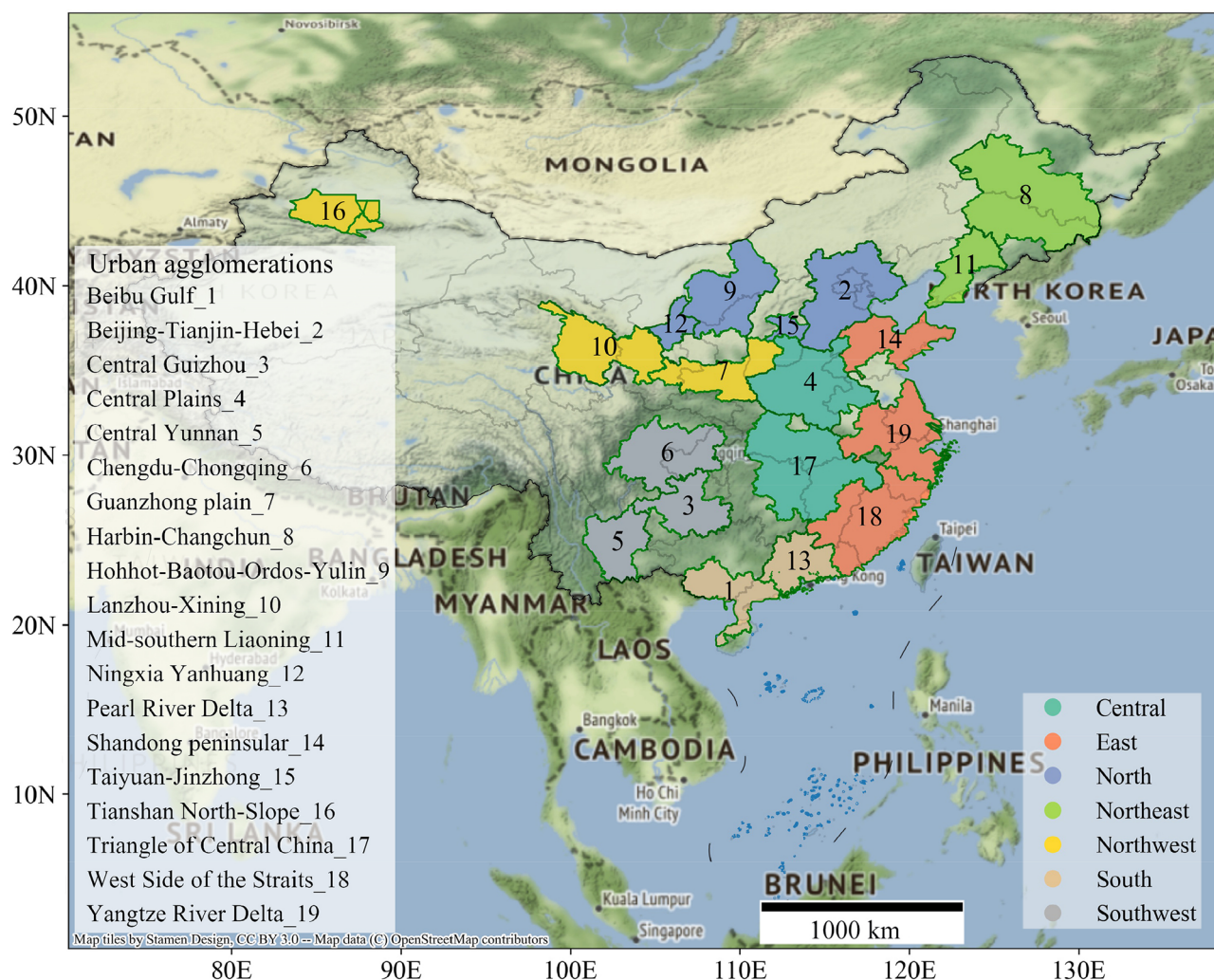
Figure 1. Geographical locations of 19 UAs in China. This figure was generated with python 3.7.6 based on geopandas and contextily packages. The scope of 19 UAs were obtained according to the Chinese planning documents. The source of the base map from contextily package is 'http://{s}.tile.stamen.com/terrain/{z}/{x}/{y}.jpg'.

the study period was conducted from January 1, 2015, to December 31, 2019, avoiding the impact of the COVID-19 epidemic. The air quality index (AQI) is a quantitative description of air quality data, which can denote the short-term air quality status and trends in a city[33]. The overall AQI represents the maximum of the sub-AQI of all pollutants, where when the AQI is higher than 50, the highest sub-AQI contributor is defined as the primary pollutant on that day[34]. The calculation of the AQI and primary pollutants is as follows:

$$IAQI_P = \frac{IAQI_{Hi} - IAQI_{Lo}}{BP_{Hi} - BP_{Lo}} \times (C_P - BP_{Lo}) + IAQI_{Lo} \tag{1}$$

$$AQI = Max\{IAQI1, IAQI2, \ldots, IAQIp, \ldots, IAQIn\} \tag{2}$$

where $IAQI_P$ is the air quality sub-index of pollutant item P. C_p is the concentration value of P. BP_{HI} and BP_{LO} are the high and low values of the pollutant concentration limit, respectively, similar to C_P[35]. $IAQI_{HI}$ and $IAQI_{LO}$ are air quality sub-indexes corresponding to BP_{HI} and BP_{LO}. After calculating the air quality sub-index of various pollutants, the maximum value is the air quality index (AQI). Primary pollutants are the largest corresponding pollutant items of $IAQI_P$.

Illustration of spatiotemporal variations in sector emissions. The emission source inventory used in the experiment is from the MEIC (Multi-resolution Emission Inventory for China) 2017 version developed by Tsinghua University, with a spatial resolution of $0.5° \times 0.5°$ (http://meicmodel.org). MEIC is a bottom-up emission inventory model based on a cloud computing platform that covers ten air pollutants and carbon dioxide emissions (SO_2, NO_x, CO, NMVOC, NH_3, $PM_{2.5}$, PM_{10}, BC, OC and CO_2) . It should be noted that the emission inventory contains the location and the amount of emission sources information, but does not establish a direct

Urban agglomeration (abbreviation)	Corecities	Level	Functions of UAs	Stations number	Key cities
Beijing-Tianjin-Hebei (BTH)[N]	Beijing, Tianjin	National	China's political and cultural center	79	13
Taiyuan-Jinzhong (TJ)[N]	Taiyuan	Local	The most dynamic economic belt in central Shanxi province	12	2
Hothot-Baotou-Ordos-Yulin (HBOY)[N]	Hothot, Ordos	Local	National high-end energy and chemical industry base	23	4
Ningxia Yanhuang (NY)[N]	Yinchuan	Local	Concentrating 90% of the urban population of Ningxia and spreading along the Yellow River	16	4
Shandong Peninsular (SP)[E]	Qingdao	Regional	The economic center of the Yellow River basin	89	14
Yangtze River Delta (YRD)[E]	Shanghai, Hangzhou	National	The leader of the Yangtze River Economic Belt	170	27
West Side of the Straits (WSS)[E]	Xiamen, Wenzhou	Regional	New comprehensive corridor for opening to the outside world along the southeast coast	88	19
Central Plain (CP)[C]	Zhengzhou	Regional	The most densely populated one with rapid industrialization and urbanization	110	28
Triangle of Central China (TCC)[C]	Wuhan	National	An essential part of the Yangtze River economic belt and a key area to promote new urbanization	138	31
Pearl River Delta (PRD)[S]	Guangzhou, Shenzhen	National	China Open and Innovation Pilot Zone	72	15
Beibu Gulf (BG)[S]	Zhanjiang	Regional	Chinese most growing coastal economic belt	41	15
Harbin-Changchun (HC)[NE]	Harbin, Changchun	Regional	Core competitiveness and essential influence in Northeast China	55	11
Mid-southern Liaoning (MSL)[NE]	Dalian, Shenyang	Regional	A region of earlier industrial development and a high level of urbanization	57	9
Central Guizhou (CG)[SW]	Guiyang	Local	Pilot demonstration area of new urbanization with mountainous characteristics	23	6
Central Yunnan (CY)[SW]	Kunming	Local	China's southwest economic growth pole	17	5
Chengdu-Chongqing (CC)[SW]	Chengdu, Chongqing	National	China's largest economy closest to Southeast and South Asia	88	16
Guanzhon gPlain (GP)[NW]	Xi'an	Regional	The second largest urban agglomeration in the western region	51	10
Lanzhou-Xining (LX)[NW]	Lanzhou, Xining	Local	A major area for national security and ecological security	19	9
Tianshan North-Slope (TNS)[NW]	Urumqi	Regional	Chinese westernmost urban agglomeration and the core area of the silk road economic belt	13	10

Table 1. Basic indicators of UAs in China. N, E, C, S, NE, SW, NW correspond to North, East, Central, South, Northeast, Southeast, Northwest.

Time(y-m-d h)	City	Site	AQI	$PM_{2.5}$ (µg/m³)	PM_{10} (µg/m³)	SO_2 (µg/m³)	NO_2 (µg/m³)	CO (mg/m³)	O_3_8h (µg/m³)
2015-01-02 01:00:00	Beijing	Olympic Sports Center	145	111	140	61	102	2.7	6
2015-01-02 02:00:00	Beijing	Olympic Sports Center	134	102	124	51	93	2.4	2
2015-01-02 03:00:00	Beijing	Olympic Sports Center	97	72	103	33	88	1.7	2
……	……	……	……	……	……	……	……	……	……
2015-01-02 01:00:00	Beijing	The temple of heaven	132	100	148	20	83	2.5	14
2015-01-02 02:00:00	Beijing	The temple of heaven	145	111	161	18	88	3	9
2015-01-02 03:00:00	Beijing	The temple of heaven	130	99	153	20	91	3.5	7
……	……	……	……	……	……	……	……	……	……

Table 2. The raw data example of cities.

relationship with ambient air quality. The emission source inventory here is mostly used as input data of various chemistry transport model[36]. Since pollutants go through a series of complex physical and chemical processes after entering the atmosphere, the contribution of various industries to the environmental concentration of pollutants is highly nonlinear and constantly changing. That is, emissions from MEIC are not equal to ground monitoring values.

The emission data are divided into five sectors: industry, power, residential, transportation and agriculture. Annual grid emission inventories of 0.25°, 0.5° and 1.0° spatial resolutions are provided. Currently, MEIC data are widely used by more than 100 research institutions and business units to forecast air quality and plan air pollution standards[36,37].

Herein, in our research, two mathematical statistical methods, including the average industrial emission of pollutants (IEP) and growth rate, were used to evaluate spatiotemporal variations in IEP in 19 UAs. The formulas of these indexes are specified as follows:
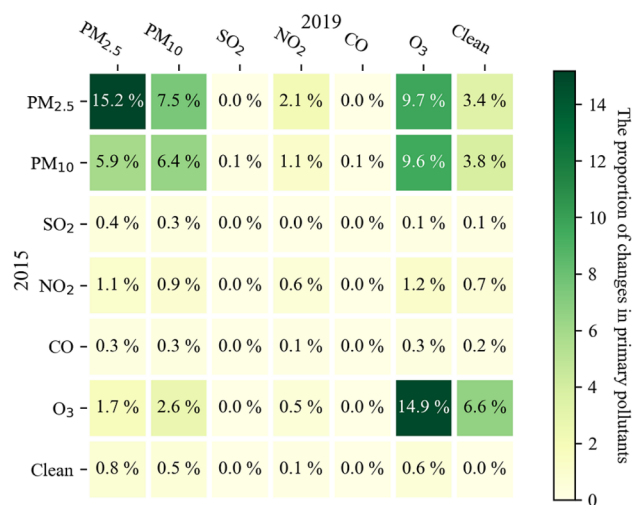
Figure 2. Transfer change matrix heatmap of primary pollutants from 2015 to 2019.

$$AI_{x,j} = \frac{1}{n} \sum_{i}^{n} IEP_{i,j} \qquad (3)$$

$$GI_{x,j} = \frac{AI_{x,j}^{2017} - AI_{x,j}^{2015}}{AI_{x,j}^{2015}} \times 100\% \qquad (4)$$

where $AI_{x,j}$ is the average industrial emission of j pollutants in city x, $IEP_{i,j}$ is the estimated *IEP* of pixel i of j pollutants, and $GI_{x,j}$ stands for the growth rate of *IEP* of j pollutants. To further explore the spatial and temporal variations in UAs, the spatial changes in the industrial emissions of pollutants at the UA scale were calculated by averaging the *AI* value in the inner city. Specific experiments were completed by zonal statistics function on ArcGIS 10.6 platform. Zoning statistical tools are also widely used in scientific researches, which can summarize the values of raster within the zones of another dataset (either raster or vector). The explanation link for this tool is as follows: https://desktop.arcgis.com/zh-cn/arcmap/latest/tools/spatial-analyst-toolbox/how-zonal-statistics-works.htm.

Besides, Mann–Kendall trend test and spatial centroid calculation were used to explore the spatiotemporal variation patterns of UAs on pollutant concentration.

Results and discussion

Daily change in primary pollutants. To elucidate the change trend of primary pollutants under the 13th Five-Year Plan, we calculated the daily primary pollutants in 2015 and 2019 based on formula (1) and formula (2). Such diurnal comparisons can reduce the effects of seasonal weather to some extent. From the 19 UAs (224 prefecture-level cities), the heat diagram of the daily change transfer matrix of primary pollutants from 2015 to 2019 is shown in Fig. 2, including six primary pollutants and clean day conditions.

From the sum of the diagonal numbers, 37% of the primary pollutants had no shift during the 13th Five-Year Plan period. $PM_{2.5}$, PM_{10} and O_3 were the main primary pollutants, especially $PM_{2.5}$. More primary pollutants were diverted to ozone pollution, indicating that the proportion of O_3 as the primary pollutant is gradually increasing. In addition, the proportion of clean air has increased significantly, which shows that pollution control has been effectively reflected during the 13th Five-Year Plan period. However, the proportion of NO_2 before and after metastasis was approximately the same, with approximately 5% NO_2 pollution. This may imply that the governance of NO_2 pollution was rendered nonsignificant. It is noteworthy that ozone pollution in China has become an increasingly prominent task in recent years. Similar to Xiao's[16] research on ozone pollution, they argue that present-day ozone levels in major Chinese cities are comparable to or even higher than the 1980 levels in the United States. Taken together, ozone and $PM_{2.5}$ have become the top two air pollution pollutants in China.

Monthly distribution of primary pollutants. To further explore the spatiotemporal distribution of the primary pollutants across the UAs, we obtained the most primary pollutants per month by dividing the number of days with the most pollutants by the number of cities in each UA from the 2019 data. In Fig. 3, the UAs location was plotted on the abscissa, and the monthly variance of the primary pollutant was plotted on the ordinate. As shown in Fig. 3, $PM_{2.5}$ appeared as dark green, PM_{10} appeared as light green, O_3 appeared as orange, NO_2 appeared as yellow, and clean days appear as dark blue. The main pollutants in the 19 UAs are $PM_{2.5}$, PM_{10} and O_3. NO_2, as the primary pollutant, only appeared in the HBOY UA in January. Ordos, located in HBOY, possess rich oil and coal resources, with coal mining as its leading industry[38]. According to the China Energy Statistical Yearbook 2019, nearly 250 million tons of raw coal were used for thermal power generation in Inner Mongolia
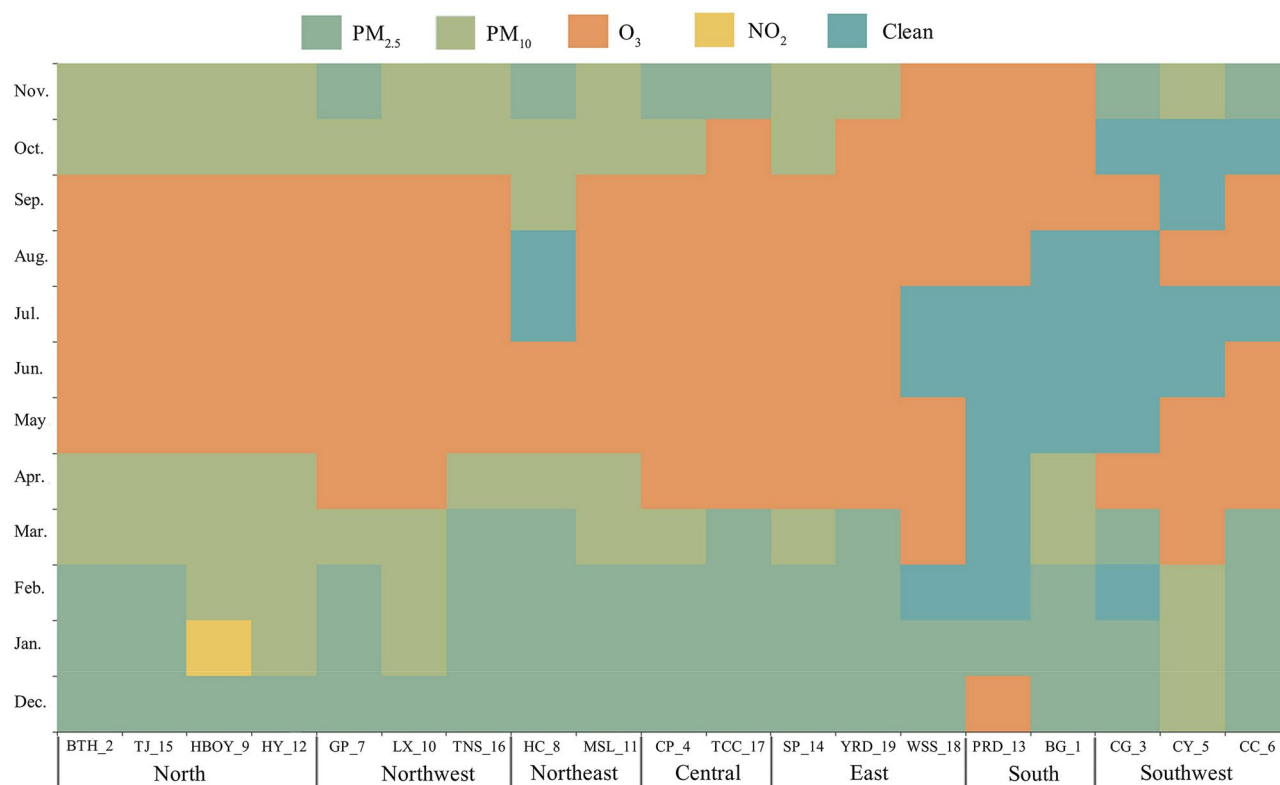
Figure 3. Monthly calendar of primary pollutants in UAs in 2019.

Autonomous Region, making it the region with the largest amount of raw coal for thermal power generation in China[39]. To a certain extent, the increase of heating[40] and the imperfect denitration technology[41] are both contributing to the increase of NO_2 pollution in the atmosphere. CO and SO_2 did not become major pollutants. Clean days (where AQI < 50) occurred mainly in South and Southwest China during summer. As the primary pollutant, $PM_{2.5}$ is mainly concentrated in December, January and February, that is, it occurs in winter. As the primary pollutant, PM_{10} is mainly concentrated in October–November and March–April, that is, autumn and spring. As the primary pollutant, O_3 is mainly concentrated from May to September, that is, summer. These results are in accord with recent studies indicating that they showed a strong seasonality but there were small differences[6,42,43].

From the perspective of UAs, monthly primary pollutants in different UAs are different[44]. The O_3 pollution in the PRD and BG, as representatives of UAs in southern China, mainly concentrated from August to November. In addition to human factors, this may be associated with lower latitudes, higher temperatures and stronger solar radiation[19,45]. The northern, northwestern, northeastern, central and eastern UAs have similar monthly primary pollutant distributions, with $PM_{2.5}$, PM_{10} and O_3 pollution distributed in the 12 months of 2019. Near surface O_3 is mainly produced by the complex photochemical reactions between nitrogen oxides, volatile organic compounds, carbon monoxide, methane and other precursors[19]. O_3 was a major pollutant in most UAs from May to September, which may be the result of the comprehensive action of anthropogenic factors and meteorological conditions.

Annual patterns of ambient air pollutants. As shown in Fig. 4, unary linear regression was used to extract the time variation trend of $PM_{2.5}$, PM_{10} and O_3 concentrations in each UA. The slope value depicted a decreasing trend in the annual mean $PM_{2.5}$ and PM_{10} during 2015–2019, suggesting that the emissions of particulate matter were effectively controlled. Meanwhile, ozone pollution has become a new environmental challenge in most UAs. The non-parametric Mann–Kendall trend test and Sen's slope estimator (MKTT-SSE) confirmed these findings (Table 3).

In more details in UAs, the average annual $PM_{2.5}$ and PM_{10} concentrations significantly decreased, mostly in the BTH, SP, PRD and CC UAs, which are economically developed regions in China[46,47] (Fig. 4, Table 3). Among them, BTH region had the largest reduction of $PM_{2.5}$ concentrations in the 10th, 12th and 13th FYP period[48]. In contrast, the annual mean ozone pollution displayed the greatest enhancement while $PM_{2.5}$ and PM_{10} showed a minimal decrease in the TJ UA in northern China. Regarding MKTT-SSE, annual mean concentration of SO_2 decreased statistically significant (P < 0.05) in most UAs, especially in TJ, which affiliated Shanxi Province, with nearly 12 μg/m³ per year during the 13th Five-Year Plan period. As reported by People's Government of Shanxi Province, the main measures to the reduction the concentration of SO_2 include the designation of "no-coal areas", raising the standard for eliminating excess capacity and increasing railway freight[49]. However, the concentration of NO_2 was still increasing with 3.10 μg/m³ per year, so it is imminent to adjust the industrial structure and control the discharge of pollutants. Regional emergency linkage can effectively deal with the heavily polluted
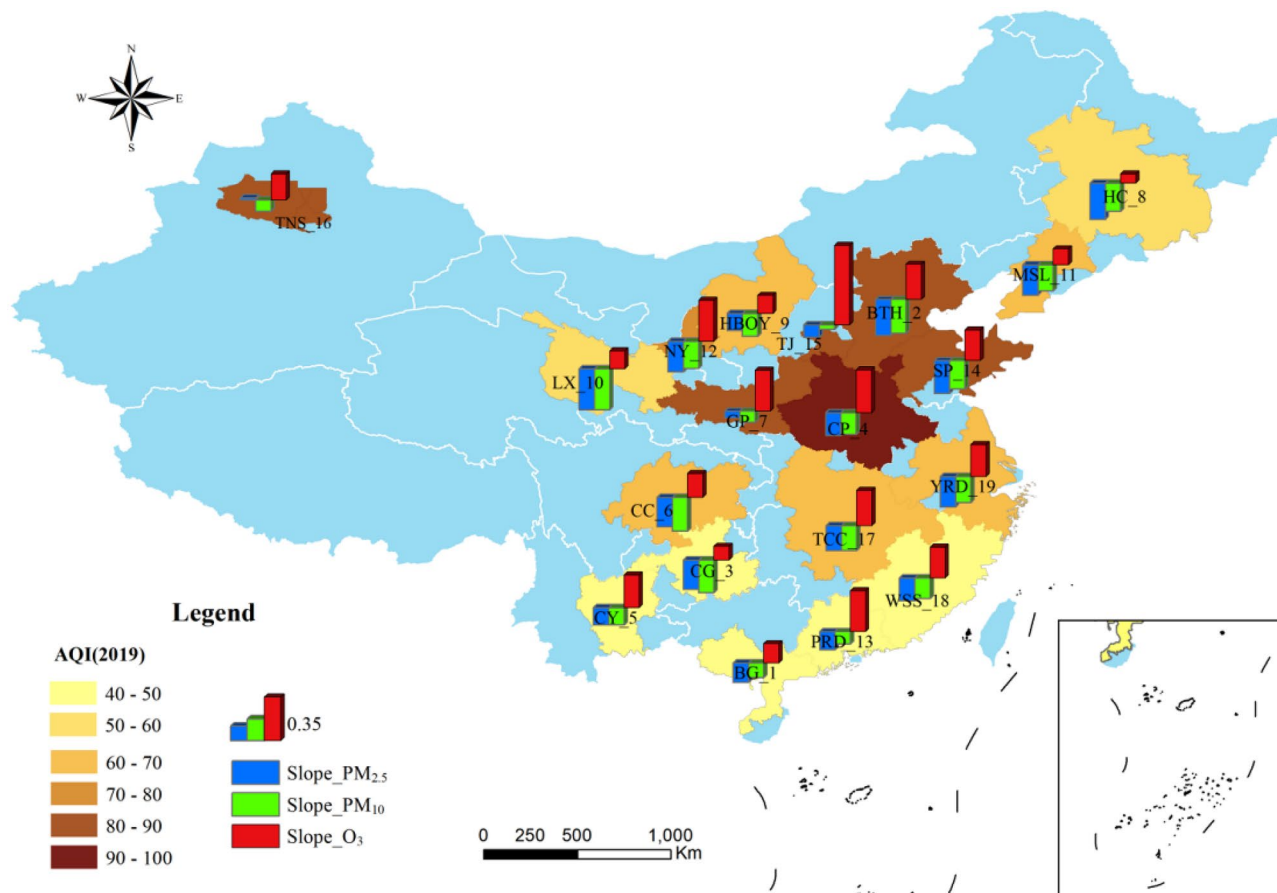
Figure 4. Annual variation trends (slope values) of three major pollutants in each UA of China from 2015 to 2019. This figure was made in the ArcGIS 10.6 platform.

UAs	PM$_{2.5}$		PM$_{10}$		NO$_2$		O$_3$		SO$_2$		CO	
	MK (z,s)	SSE	MK (z,s)	SSE	MK (z,s)	SSE	MK (z,s)	SSE	MK (z,s)	SSE	MK (z,s)	SSE
BTH_2	−2*	−6.93	−2*	−10.07	−1	−2.97	2	3.04	−2	−6.78	−2*	−0.14
TJ_15	−1	−2.88	0	1.53	1	3.10	2	4.31	−2	−11.98	−2	−0.14
HBOY_9	−2	−1.21	0	−2.85	1	0.40	0	0.40	−2*	−2.64	−2	−0.08
NY_12	−2	−3.71	0	−3.46	1	1.12	1	2.30	−2	−8.32	−2*	−0.04
SP_14	−2	−7.99	−2*	−10.20	−2	−1.47	1	2.77	−2*	−7.93	−2*	−0.14
YRD_19	−2*	−3.50	−2	−4.65	−1	−0.64	1	1.34	−2*	−3.27	−2*	−0.05
WSS_18	−2*	−1.79	−2*	−1.97	−1	−0.71	1	1.89	−2*	−1.37	−2*	−0.04
CP_4	−2*	−4.50	−2*	−6.21	−1	−1.78	2	4.05	−2*	−7.04	−2	−0.17
TCC_17	−2	−3.16	−2*	−4.74	0	−0.26	2*	1.83	−2	−3.09	−2	−0.05
PRD_13	−1	−1.21	−1	−1.09	0	0.02	2*	1.72	−2*	−1.06	−2	−0.04
BG_1	−2	−1.17	−2*	−1.00	0	−0.05	1	0.62	−1	−0.45	−2*	−0.03
HC_8	−1	−3.95	−1	−5.09	−2*	−1.98	0	0.09	−2*	−3.65	−1	−0.05
MSL_11	−2	−4.02	−2	−5.62	−2*	−1.17	0	0.13	−2*	−4.94	−2*	−0.07
CG_3	−2	−2.22	−2	−3.36	−2	1.33	0	0.17	−2*	−1.52	−2	−0.04
CY_5	−2	−1.26	−1	−2.34	0	0.17	1	1.56	−2*	−2.43	−2	−0.05
CC_6	−2	−4.21	−2*	−7.67	1	0.12	0	0.93	−2*	−2.38	−2*	−0.05
GP_7	−1	−2.84	−1	−2.83	0	−0.14	1	2.27	−2	−5.89	−2	−0.17
LX_10	−2*	−4.14	−2	−6.96	−2	−0.62	0	−0.06	−2*	−2.48	−2*	−0.03
TNS_16	0	−0.27	0	1.74	0	0.17	0	1.05	−2	−1.36	−1	−0.13

Table 3. MKTT-SSE for annual mean concentration of air pollutants in 19 UAs from 2015 to 2019. *P < 0.05. *MK* Mann–Kendall trend, *SSE* Sen's slope estimate. The unit of SSE is concentration/year. Concentration: μg/m³ for PM$_{10}$, PM$_{2.5}$, O$_3$, NO$_2$ and SO$_2$, and mg/m³ for CO.

Pollutants	Averaging time	GB3095-2012		AQG 2021				AQG
		Level-1	Level-2	IT-1	IT-2	IT-3	IT-4	
PM$_{2.5}$ (µg/m^3)	Annual	15	35	35	25	15	10	5
PM$_{10}$ (µg/m^3)	Annual	40	70	70	50	30	20	10

Table 4. Recommended AQG levels and interim targets.
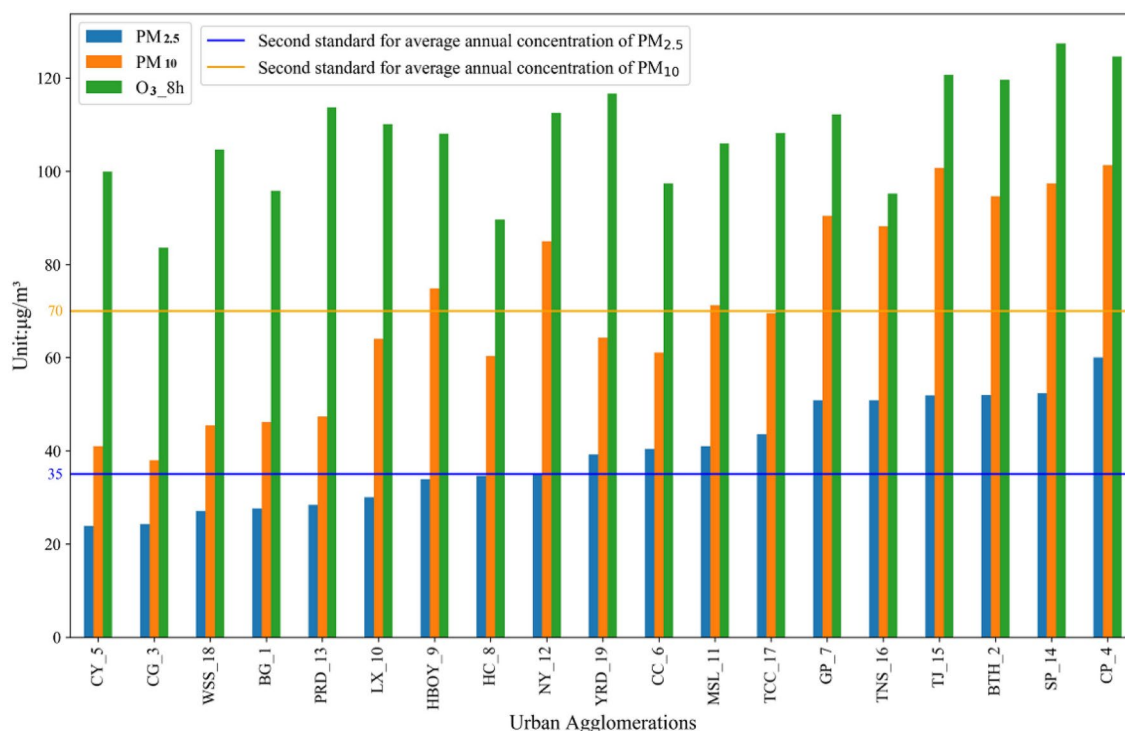
**Figure 5.** Numerical distribution of three major pollutant concentrations in UAs in 2019.

weather. For CO pollution, it decreased statistically significant (P < 0.05) with the slope of 0.07 mg/m^3 per year in all UAs (Table 4).

At the same time, by checking the annual average AQI in 2019, we showed that the CP UA has the highest annual average AQI, and the particulate matter pollution and ozone are both high, suggesting that the control effect is not obvious in the central region. We found that the annual average AQI showed a gradually decreasing trend outward, taking the CP UA as the center. In addition, the UAs in the southern and southwestern regions showed both good annual average AQI and low fine particulate pollution while high ozone concentration pollution. The average annual AQI, fine particulate matter and ozone pollution in the TNS are also at a high level in 19 UAs. This is consistent with the level of the monthly primary pollutants mentioned above.

The World Health Organization (WHO) published new Global Air Quality Guidelines (AQGs), which recommend new air quality levels on 22 September 2021. As shown in Table 4 and Fig. 5, almost half of the UAs have reached the second-level national standards of China and the first-stage interim target of the World Health Organization.

Hourly variations in PM$_{2.5}$, PM$_{10}$ and O$_3$. As seen from the above analysis, the spatial distribution of changes and the concentrations of air pollutants shared a location similarity between adjacent UAs. Furthermore, to profile the diurnal changes in pollutant concentrations during the 13th Five-Year Plan, the 24-hourly variations were calculated in seven directions. The results are shown in Fig. 6. From 2015 to 2019, the rates of O$_3$ concentration in any hour significantly increased compared to particulate matter (PM) pollution, which was consistent with the average annual variation trends above. Overall, diurnal trends in O$_3$ concentration at UAs in all directions also showed a single peak, with the largest increments concentrating between 13:00 and 16:00, due to more frequent heat waves in recent times[50] and the fact that higher temperature, lower relative humidity, and stronger solar radiation at 16:00 favor more secondary pollutant production[9,51]. A similar hourly variation, which daytime O$_3$ increased more significantly than that of nighttime in Beijing, has been reported[5]. However, the peak O$_3$ pollution spatially varied, exhibiting a relatively earlier trend in the southeastern region than in the northwestern region because of the Earth's rotation, making the eastern area receive direct sunlight first. The dis-
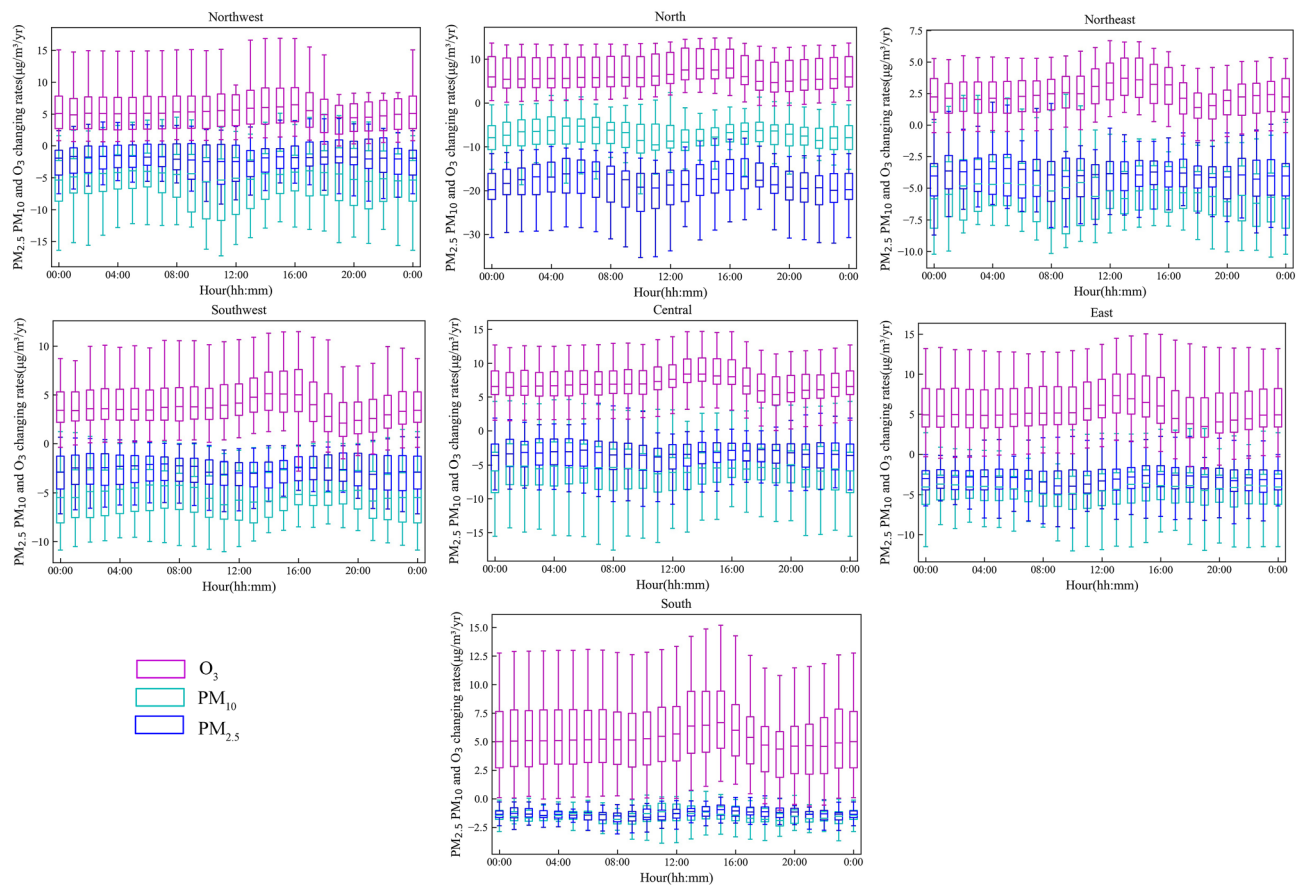
Figure 6. Box plots of hourly three major pollutant rates across UAs.

tance between the whiskers of the box plot in the southern city is the largest compared with the others, indicating that ground-level ozone concentration variations presented great dissimilarity in southern cities.

For PM pollution, there was a significant downward trend in all UAs. $PM_{2.5}$ reduction is more obvious in rush hours (10:00 and 22:00), which reveals the response to aggressive actions by the government to restrict motor vehicles[51]. In addition, we noticed that the 'coal-to-gas and coal-to-electricity' transformation has substantially improved air pollution, particularly in northern China. It seems clear from these figures that the changing rate of $PM_{2.5}$ in northern regions was significantly higher than that of PM_{10}.

Spatial centroid variations of air pollutants. As far as pollution centroid are concerned, their trends indicate that the ambient air pollutants are gradually moving southward and mainly concentrated in the Central Plains UA from 2015 to 2019 (Fig. 7). We noticed that the centroids of $PM_{2.5}$ and PM_{10} showed similar movement trends, which were both firstly located in the north of the Zhumadian city in Henan Province, and following to the southwest sharply about 30 km, and then slightly shifted towards the southeast, and finally located in the south of the starting centroid. In other words, PM pollution have moved towards the south during China's 13th Five-Year Plan period, indicating that the north/northeast/northwest UAs have dropped significantly than that in the southern UAs. Consistent with the results of the Shi et al. (2019), our results show that the PM governance in China is indeed effective[52] (Fig. 7a).

With respect to the SO_2 and NO_2 pollution, they were offset southwest by nearly 100 and 50 km, respectively (Fig. 7b). These two pollutants have the largest offset, which may suggest that the decline of SO_2 and NO_2 pollution in northeast is greater than that of other pollutants. These findings have also been evidenced by Zhang et al. (2019)[49] and Cui et al. (2021)[53].

With regard to the O_3 pollution, the centroid spatial movement trend was weak and mainly located in the north of Xinyang city in Henan Province. During the 13th Five-Year Plan period, the control of ozone pollution is not obvious. Therefore, ozone pollution become the focus of the 14th Five-Year Plan exceeded $PM_{2.5}$[54]. In term of CO pollution, it moved sharply south in 2017, indicating that CO pollution in the north has been effectively controlled since 2017 (Fig. 7c).

Sector emission source impacts on primary pollutants. Due to the availability of data, statistics on industry emissions are limited to 2015–2017. The average annual emission value of agricultural sources was too small to provide statistical significance. Figure 8 only shows the contribution of four sector sources (industry, power, residential and transportation) to pollutants in 19 UAs from 2015 to 2017, where the dotted line repre-
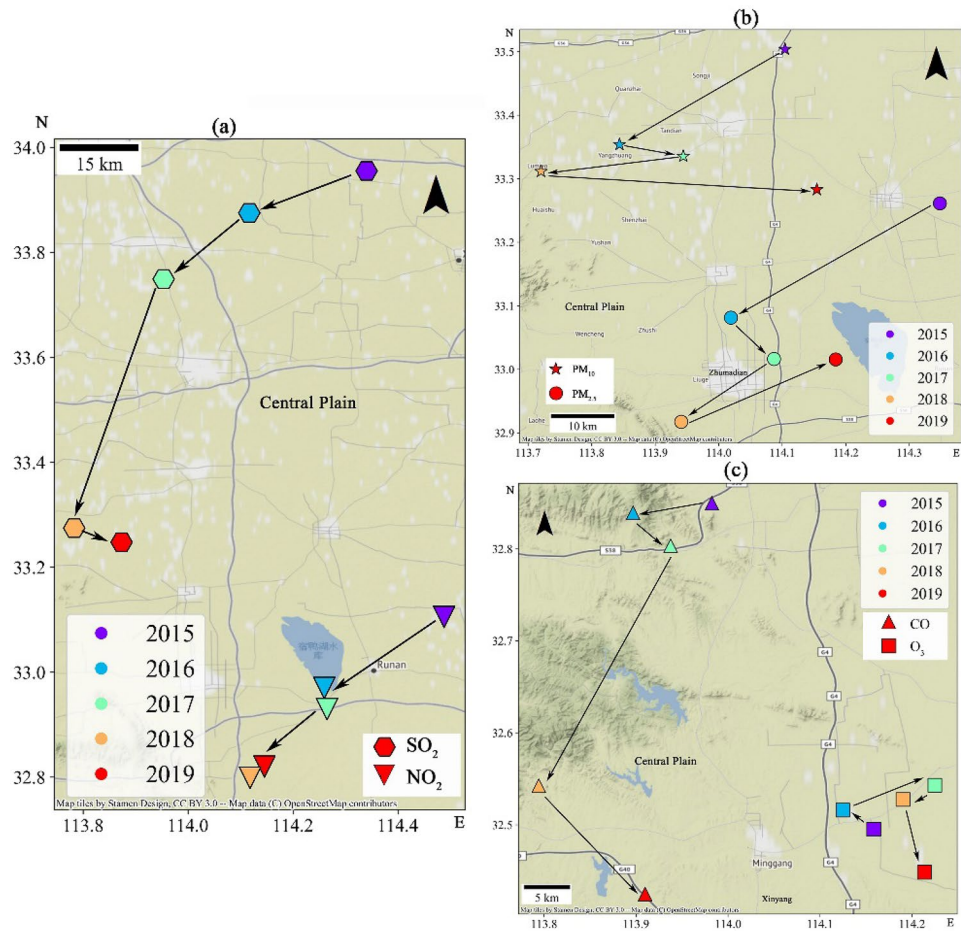
Figure 7. Moving path of the centroids of six air pollutants. (We marked the centroid of $PM_{2.5}$ pollution with circle, PM_{10} with star, O_3 with square, CO with triangle_up, NO_2 with triangle_down and SO_2 with hexagon.). This figure was generated with python 3.7.6 based on geopandas and contextily packages. The source of the base map from contextily package is 'http://{s}.tile.stamen.com/terrain/{z}/{x}/{y}.jpg'.
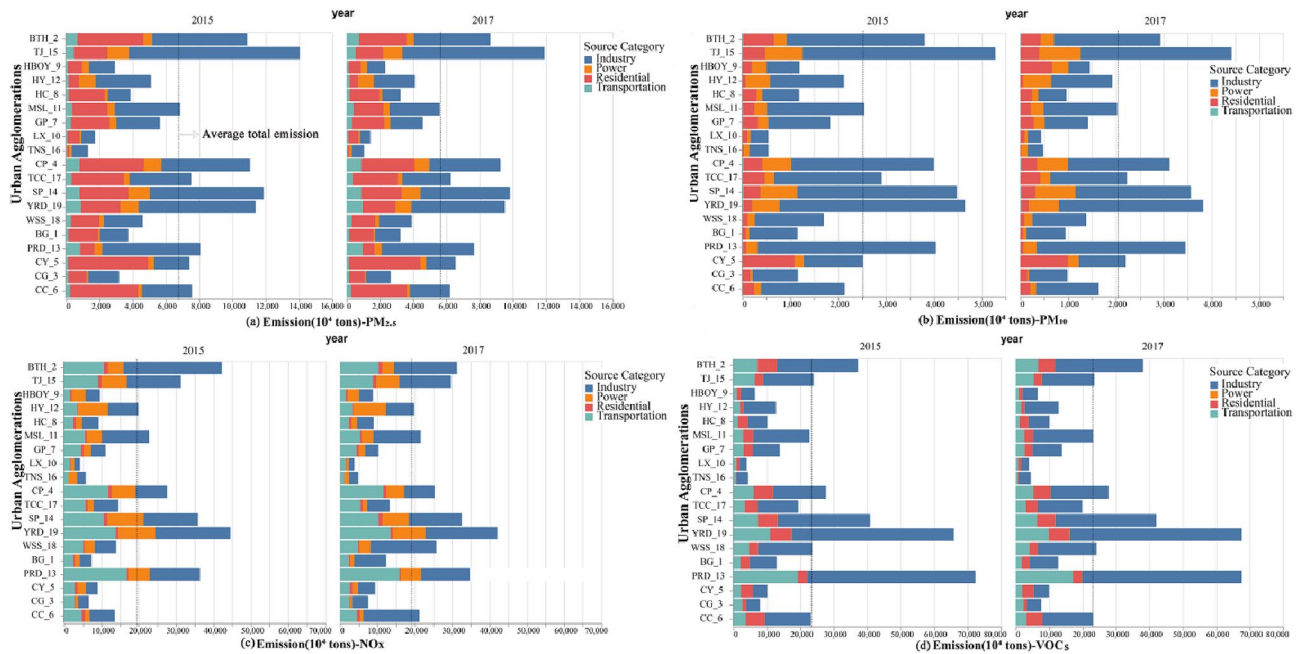
Figure 8. Average sector emission of pollutants in 19 UAs.

sents the average of total emissions. As a result, near-surface ozone pollution is a secondary pollutant produced by the photochemical reaction of a series of precursors under the action of solar radiation. In particular, VOCs and NO_x are important precursors for ozone pollution[19]. Therefore, we explore the emissions of these two important precursors in different UAs.

Sector pollution sources directly cause increases in $PM_{2.5}$, PM_{10}, nitrogen oxides, volatile organic compounds and other pollutants in the atmosphere[55]. As seen from Fig. 8a, $PM_{2.5}$ is mainly derived from industrial sources, and the main high value areas are TJ, YRD and SP UAs. Meanwhile, in the three UAs, the total contribution of anthropogenic emission sources to particulate pollution declined the fastest, which is largely related to government intervention, industrial transformation and environmental governance. Approximately 50–75% of $PM_{2.5}$ in the northern UAs comes from industrial sources, while $PM_{2.5}$ in the southwestern UAs mainly comes from residential sources. This result is similar to the analysis of $PM_{2.5}$ sources in BTH in 2013 by Li et al. Regarding PM_{10}, industrial sources have the greatest influence on PM_{10} in all UAs (Fig. 8b). There is no significant regional difference in the impact of traffic sources on $PM_{2.5}$ and PM_{10}. The contribution of traffic sources to $PM_{2.5}$ in 19 UAs is 5–7% on average, and PM_{10} tends to 0. By using the receptor model method, Huang et al.[56] found that the contribution of gasoline dust to total suspended particulate matter (TSP) in Changzhou was less than 1%, confirming that exhaust gas was not the main contribution source of $PM_{2.5}$. In each UA, the cumulative emission of $PM_{2.5}$ is consisted of the four average emissions caused by anthropogenic sources, which is approximately 2.5 times of that of PM_{10} (Fig. 8a,b). Here the emissions of pollutants from different sources were calculated, and the cumulative emission were all decreasing. However, we did not use the atmospheric transmission model to simulate pollutant concentration, so different from Zhang's research[57] on PRD, we could not get how various control measures and policies affect the monitoring concentration of different urban agglomerations.

Among the 19 UAs, NO_x and VOCs mainly come from industrial and traffic sources, with less contribution from residential and power sources (Fig. 8c,d). During the study period, the NO_x emissions of most UAs decreased, but the CY, CG and CC UAs in the southwest, WSS in the eastern and BG UAs all showed an increasing trend of NO_x. This is mainly concentrated in the increase in industrial sources, which can also be seen from the increase in industrial production in the south. The contribution rate of power sources to VOCs in UAs is low and can be ignored.

From the perspective of time series changes, the contribution rate of anthropogenic emission sources to particulate pollution is decreasing, but for gas pollutants, nearly half of UAs show an increasing trend of VOCs and NO_X. In addition, VOCs high value areas are mainly concentrated in the YRD, PRD, BTH and other state-level UAs. In regional joint prevention and control, different UAs have different priorities to prevent and control sector emission of pollutants.

Limitations of this study. As mentioned in the literature reviews, air pollution is not only affected by social activities and atmospheric emissions, but also by the impacts of meteorological factors[6,44]. In previous studies, we have specially studied the impact of meteorological elements on the YRD UA and found that the winds blowing to YRD (southeasterly & northwesterly) have opposite effects on air quality. This study only visualized the emission source inventory of pollutants at urban agglomeration scale. A number of work remain to be done in future research. Meteorological factors (temperature, wind speed, wind direction and etc.[58,59]) and chemistry transport model (such as integrated source apportionment method[60–62]) were not taken into account, so the contribution of anthropogenic sources to air pollutant concentration and trans-regional transmission of pollution were not realized in this study. Thus, it is necessary to further explore the impact of the combination of social and meteorological activities on air pollution.

Conclusions

Other studies conducted on the temporal and spatial variations in air primary pollutants in 19 UAs during the 13th Five-Year Plan are not sufficient. Based on air quality monitoring data and using mathematical statistics and cartography, this paper analyzed the spatiotemporal characteristics of primary pollutants over 19 Chinese UAs. Although we have achieved remarkable results in pollution control during the 13th Five-Year Plan period, PM and O_3 pollution are still serious problems in China. Returning to the question posed at the beginning of this study, it is now possible to state that the main conclusions are as follows:

(1) Generally, from the daily changes of all primary pollutants, 37% of the primary pollutants had no shift during the 13th Five-Year Plan period. $PM_{2.5}$, PM_{10} and O_3 were the main primary pollutants, especially $PM_{2.5}$. The proportion of clean air days has increased significantly. NO_2 pollution was rendered nonsignificant.

(2) From the perspective of monthly distribution of primary pollutants, clean days (where AQI < 50) occur mainly in South and Southwest China during summer. As the primary pollutant, $PM_{2.5}$ is primarily concentrated in December, January and February, and PM_{10} is primarily concentrated in October–November and March–April. The O_3 pollution in the PRD and BG is mainly concentrated from August to November. The northern, northwestern, northeastern, central and eastern UAs have similar monthly primary pollutant distributions.

(3) In terms of air quality differences in UAs, the annual average AQI showed a gradually decreasing trend outward, taking the Central Plain as the center. The Central Plain has the highest annual average AQI, and

the particulate matter pollution and ozone are both high, suggesting that the control effect is not obvious in the central region. The average annual $PM_{2.5}$ and PM_{10} concentrations decreased, most significantly in HC and MSL in the northeast, while there was little difference in annual ozone concentration. In contrast, the annual mean ozone pollution displayed the greatest enhancement, while $PM_{2.5}$ and PM_{10} showed a minimal decrease in TJ UA in northern China. BTH UA had the largest reduction of $PM_{2.5}$ concentration and the ambient air pollutants are gradually moving southward and mainly concentrated in the Central Plain from 2015 to 2019.

(4)   There were significant differences in the intensity and direction of each sector emission source in nineteen UAs. The total amount of PM discharged from the emission sources of Taiyuan-Jinzhong, Yangtze River Delta and Shandong Peninsular was much higher than those of others. $PM_{2.5}$ and PM_{10} are mainly derived from industrial sources. The contribution rate of anthropogenic emission sources to particulate pollution is decreasing, but for gas pollutants, nearly half of UAs show an increasing trend of VOCs and NO_X.

Based on the above findings, this paper proposes the following policy recommendations. First, it is necessary to pay more attention to emission reduction efforts in national UAs. Second, PM and ozone pollution are important pollution types in UAs in China, and they should be coordinated in prevention and control. The government should strengthen regional joint prevention and control and establish a compensation and incentive mechanism for cities with weak economies. Third, different UAs should formulate differentiated PM and O_3 emission reduction strategies according to their own social and economic conditions. Industrial emissions are still an important source of air pollution, and the industrial structure should be optimized based on local resources. We will encourage energy enterprises to develop energy and introduce new energy technologies. We will improve cleaner production technology and build a monitoring platform for urban greening.

Data availability
Data and materials are available from the authors upon request.

References
 1. Khaniabadi, Y. O. *et al.* Exposure to PM10, NO2, and O3 and impacts on human health. *Environ. Sci. Pollut. Res.* **24**, 1–9 (2017).
 2. Hu, F. & Guo, Y. Health impacts of air pollution in China. *Front. Environ. Sci. Eng.* **15**, 18. https://doi.org/10.1007/s11783-020-1367-1 (2021).
 3. Zhang, H., Chen, J. & Wang, Z. Spatial heterogeneity in spillover effect of air pollution on housing prices: Evidence from China. *Cities* **113**, 103145 (2021).
 4. Faridi, S., Niazi, S., Yousefian, F., Azimi, F. & Naddafi, K. Spatial homogeneity and heterogeneity of ambient air pollutants in Tehran. *Sci. Total Environ.* **697**, 134123 (2019).
 5. Chen, S., Wang, H., Lu, K., Zeng, L. & Zhang, Y. The trend of surface ozone in Beijing from 2013 to 2019: Indications of the persisting strong atmospheric oxidation capacity. *Atmos. Environ.* **242**, 117801 (2020).
 6. Zhao, S., Yin, D., Yu, Y., Kang, S. & Dong, L. PM2.5 and O3 pollution during 2015–2019 over 367 Chinese cities: Spatiotemporal variations, meteorological and topographical impacts. *Environ. Pollut.* **264**, 114694 (2020).
 7. Huang, C., Liu, K. & Zhou, L. Spatio-temporal trends and influencing factors of PM2.5 concentrations in urban agglomerations in China between 2000 and 2016. *Environ. Sci. Pollut. Res.* **28**, 10988–11000 (2021).
 8. Ouyang, X., Wei, X., Li, Y., Wang, X. C. & Kleme, J. Impacts of urban land morphology on PM2.5 concentration in the urban agglomerations of China. *J. Environ. Manag.* **283**, 112000 (2021).
 9. Zhao, S., Yu, Y., Qin, D., Yin, D. & He, J. Assessment of long-term and large-scale even-odd license plate controlled plan effects on urban air quality and its implication. *Atmos. Environ.* **170**, 82–95. https://doi.org/10.1016/j.atmosenv.2017.09.041 (2017).
10. Gottmann, J. Megalopolis or the urbanization of the northeastern seaboard. *Econ. Geogr.* **33**, 189. https://doi.org/10.2307/142307 (1957).
11. Zhang, Q., Jia, S., Yang, L., Krishnan, P. & Wang, X. New particle formation (NPF) events in China urban clusters given by sever composite pollution background. *Chemosphere* **262**, 127842 (2020).
12. Rahnama, M. R. Simulation of land use land cover change in Melbourne metropolitan area from 2014 to 2030: Using multilayer perceptron neural networks and Markov chain model. *Aust. Plan.* **21**, 1–14 (2021).
13. Fu, Y. & Zhang, X. Mega urban agglomeration in the transformation era: Evolving theories, research typologies and governance. *Cities* **105**, 102813 (2020).
14. Burger, M. J., Meijers, E. J. & Van Oort, F. G. Multiple perspectives on functional coherence: Heterogeneity and multiplexity in the Randstad. *Tijdschr. Econ. Soc. Geogr.* **105**, 444–464 (2015).
15. Zerboni, A. *et al.* The Khartoum-Omdurman conurbation: A growing megacity at the confluence of the Blue and White Nile Rivers. *J. Maps* **17**, 1–14 (2020).
16. Xiao, K., Wang, Y., Wu, G., Fu, B. & Zhu, Y. Spatiotemporal characteristics of air pollutants (PM10, PM2.5, SO2, NO2, O3, and CO) in the inland basin city of Chengdu, southwest China. *Atmosphere* **9**, 74. https://doi.org/10.3390/atmos9020074 (2018).
17. Luo, Y., Liu, S., Che, L. N. & Yu, Y. Analysis of temporal spatial distribution characteristics of PM2.5 pollution and the influential meteorological factors using Big Data in Harbin, China. *J. Air Waste Manag.* **71**, 964–973 (2021).
18. Yousefian, F. *et al.* Temporal variations of ambient air pollutants and meteorological influences on their concentrations in Tehran during 2012–2017. *Sci. Rep.-Uk* **10**, 1–11 (2020).
19. Li, J., Gao, Y. & Huang, X. The impact of urban agglomeration on ozone precursor conditions: A systematic investigation across global agglomerations utilizing multi- source geospatial datasets. *Sci. Total Environ.* **704**, 135458.135451-135458.135411 (2020).
20. Xu, Y. *et al.* Spatial and temporal variations in criteria air pollutants in three typical terrain regions in Shaanxi, China, during 2015. *Air Qual. Atmos. Health* **11**, 95–109 (2018).
21. Li, Y. Q., Chen, Y. L., Karimian, H. & Tao, T. H. Spatiotemporal analysis of air quality and its relationship with meteorological factors in the Yangtze River Delta. *J. Elementol.* **25**, 1059–1075. https://doi.org/10.5601/jelem.2019.24.4.1931 (2020).
22. Cheng, Y. *et al.* Humidity plays an important role in the PM2.5 pollution in Beijing. *Environ. Pollut.* **197**, 68–75 (2015).

23. Chen, J. Y., Shan, M., Xia, J. J. & Jiang, Y. Effects of space heating on the pollutant emission intensities in "2+26" cities. *Build Environ.* **175**, 106821 (2020).
24. Ai, H., Guan, M., Feng, W. & Li, K. Influence of classified coal consumption on PM2.5 pollution: Analysis based on the panel cointegration and error-correction model. *Energy* **215**, 119108 (2021).
25. Ren, Y., Wei, J., Wu, Z., Ji, Y. & Li, H. Chemical components and source identification of PM2.5 in non-heating season in Beijing: The influences of biomass burning and dust. *Atmos. Res.* **251**, 105412 (2020).
26. Tainio, M., Andersen, Z. J., Nieuwenhuijsen, M. J., Hu, L. & Sá, T. Air pollution, physical activity and health: A mapping review of the evidence. *Environ. Int.* **147**, 105954 (2021).
27. Xue, W., Zhang, J., Zhong, C., Li, X. & Wei, J. S. PM2.5 variations and its response to the industrial structure from 2000 to 2018 in the Beijing-Tianjin-Hebei region. *J. Clean. Prod.* **279**, 123742. https://doi.org/10.1016/j.jclepro.2020.123742 (2021).
28. Yan, J., Tao, F., Zhang, S., Lin, S. & Zhou, T. Spatiotemporal distribution characteristics and driving forces of PM2.5 in three urban agglomerations of the Yangtze river economic belt. *Int. J. Environ. Res. Public Health* **18**, 2222. https://doi.org/10.3390/ijerph1805 2222 (2021).
29. Zhang, R. *et al.* Chemical characterization and source apportionment of PM2.5 in Beijing: Seasonal perspective. *Atmos. Chem. Phys.* **13**, 7053–7074 (2014).
30. Monforte, P. & Ragusa, M. A. Evaluation of the air pollution in a Mediterranean region by the air quality index. *Environ. Monitor. Assess.* **190**, 1–10 (2018).
31. Shen, Y. *et al.* Spatiotemporal patterns of recent PM2.5 concentrations over typical urban agglomerations in China. *Sci. Total Environ.* **655**, 13–26 (2019).
32. Benchrif, A., Wheida, A., Tahri, M., Shubbar, R. M. & Biswas, B. Air quality during three covid-19 lockdown phases: AQI, PM2.5 and NO2 assessment in cities with more than 1 million inhabitants. *Sustain. Cities Soc.* **74**, 103170 (2021).
33. Tian, X., Cui, K., Sheu, H. L., Hsieh, Y. K. & Yu, F. Effects of rain and snow on the air quality index, PM2.5 levels, and dry deposition flux of PCDD/Fs. *Aerosol Air Qual. Res.* **21**, 210158 (2021).
34. She, Q. *et al.* Air quality and its response to satellite-derived urban form in the Yangtze River Delta, China. *Ecol. Indic.* **75**, 297–306 (2017).
35. Liu, H. M. *et al.* The effect of natural and anthropogenic factors on haze pollution in Chinese cities: A spatial econometrics approach. *J. Clean. Prod.* **165**, 323–333 (2017).
36. Zheng, B. *et al.* Trends in China's anthropogenic emissions since 2010 as the consequence of clean air actions. *Atmos. Chem. Phys.* **18**, 14095–14111. https://doi.org/10.5194/acp-2018-374 (2018).
37. Li, *et al.* Anthropogenic emission inventories in China: A review. *Natl. Sci. Rev.* **95**, 266 (2017).
38. Zheng, J. Industrial structure evolution during the industrialization process in Ordos. *J. Arid Land Resour. Environ.* **26**, 7 (2012).
39. Hussain, R. & Luo, K. Geochemical evaluation of enrichment of rare-earth and critical elements in coal wastes from Jurassic and Permo-Carboniferous coals in Ordos Basin, China. *Nat. Resour. Res.* **29**, 1731–1754 (2020).
40. Chen, L. *et al.* A land use regression for predicting NO2 and PM10 concentrations in different seasons in Tianjin region, China. *J. Environ. Sci.* **22**, 1364–1373 (2010).
41. Zhang, Y. *et al.* Aspen Plus-based simulation of a cement calciner and optimization analysis of air pollutants emission. *Clean Technol. Environ. Policy* **13**, 459–468 (2011).
42. Xu, Y. *et al.* Spatial and temporal variations in criteria air pollutants in three typical terrain regions in Shaanxi, China, during 2015. *Air Qual. Atmos. Health* **11**, 95 (2017).
43. Xiao, L. *et al.* Severe surface ozone pollution in China: A global perspective. *Environ. Sci. Technol.* **5**, 487–494 (2018).
44. Wu, Q., Guo, R., Luo, J. & Chen, C. Spatiotemporal evolution and the driving factors of PM2.5 in Chinese urban agglomerations between 2000 and 2017. *Ecol. Indic.* **125**, 107491 (2021).
45. David, L. M. & Nair, P. R. Tropospheric column O3 and NO2 over the Indian region observed by ozone monitoring instrument (OMI): Seasonal changes and long-term trends. *Atmos. Environ.* **65**, 25–39 (2013).
46. Wang, L. *et al.* Predicted impact of thermal power generation emission control measures in the Beijing-Tianjin-Hebei region on air pollution over Beijing, China. *Sci. Rep.-Uk* **8**, 934 (2018).
47. Nagashima, F. Critical structural paths of residential PM2.5 emissions within the Chinese provinces. *Energy Econ.* **70**, 465–471 (2018).
48. Lin, C. Q. *et al.* High-resolution satellite remote sensing of provincial PM 2.5 trends in China from 2001 to 2015. *Atmos. Environ.* **180**, 110–116 (2018).
49. Zhang, H., Di, B., Liu, D., Li, J. & Zhan, Y. Spatiotemporal distributions of ambient SO2 across China based on satellite retrievals and ground observations: Substantial decrease in human exposure during 2013–2016. *Environ. Res.* **179**, 108795 (2019).
50. Su, Q. & Dong, B. Projected near-term changes in three types of heat waves over China under RCP4.5. *Clim. Dyn.* **53**, 3751 (2019).
51. Wang, T. *et al.* Ozone pollution in China: A review of concentrations, meteorological influences, chemical precursors, and effects. *Sci. Total Environ.* **575**, 1582–1596 (2017).
52. Shi, C., Guo, F. & Shi, Q. Ranking effect in air pollution governance: Evidence from Chinese cities. *J. Environ. Manag.* **251**, 109600 (2019).
53. Cui, Y., Wang, L., Jiang, L., Liu, M. & Duan, X. Dynamic spatial analysis of NO2 pollution over China: Satellite observations and spatial convergence models. *Atmos. Pollut. Res.* **12**, 89 (2021).
54. Zhou, W., Chen, C., Lei, L., Fu, P. & Sun, Y. Temporal variations and spatial distributions of gaseous and particulate air pollutants and their health risks during 2015–2019 in China. *Environ. Pollut.* **272**, 116031 (2020).
55. Zheng, B., Cheng, J., Geng, G., Wang, X. & He, K. Mapping anthropogenic emissions in China at 1 km spatial resolution and its application in air quality modeling. *Sci. Bull.* **66**, 612 (2020).
56. Huang, S. *et al.* Sources of aerosol partcales in Changzhou city. *J. Meteorol. Sci.* **15**, 9 (1995) (**(in Chinese)**).
57. Zhang, X., Fung, J., Zhang, Y., Lau, A. & Huang, W. W. Assessing PM2.5 emissions in 2020: The impacts of integrated emission control policies in China. *Environ. Pollut.* **263**, 114575 (2020).
58. Qi, Y., Li, W. & Zhang, H. Local and inter-regional contributions to PM2.5 nitrate and sulfate in China. *Atmos. Environ.* **94**, 582–592 (2014).
59. Zhong, Q. *et al.* Distinguishing emission-associated ambient air PM2.5 concentrations and meteorological factor-induced fluctuations. *Environ. Sci. Technol.* **52**, 10416–10425 (2018).
60. Zhang, H. Y., Cheng, S. Y., Yao, S., Wang, X. Q. & Wang, C. D. Insights into the temporal and spatial characteristics of PM2.5 transport flux across the district, city and region in the North China Plain. *Atmos. Environ.* **218**, 117010 (2019).
61. Heo, J., Adams, P. J. & Gao, H. O. Public health costs of primary PM2.5 and inorganic PM2.5 precursor emissions in the United States. *Environ. Sci. Technol.* **50**, 6061 (2016).
62. Zhai, *et al.* Detection of critical PM2.5 emission sources and their contributions to a heavy haze episode in Beijing, China, using an adjoint model. *Atmos. Chem. Phys.* **580**, 284 (2018).

Competing interests

The authors declare no competing interests.

Additional information

Correspondence and requests for materials should be addressed to Y.S.

Reprints and permissions information is available at www.nature.com/reprints.

Publisher's note Springer Nature remains neutral with regard to jurisdictional claims in published maps and institutional affiliations.